

# Generalized harmonic spatial coordinates and hyperbolic shift conditions

Miguel Alcubierre,<sup>1</sup> Alejandro Corichi,<sup>1</sup> José A. González,<sup>2</sup> Darío Núñez,<sup>1</sup> Bernd Reimann,<sup>1,3</sup> and Marcelo Salgado<sup>1</sup>

<sup>1</sup>*Instituto de Ciencias Nucleares, Universidad Nacional Autónoma de México, A.P. 70-543, México D.F. 04510, México*

<sup>2</sup>*Theoretical Physics Institute, University of Jena, Max-Wien-Platz 1, 07743, Jena, Germany*

<sup>3</sup>*Max Planck Institut für Gravitationsphysik, Albert Einstein Institut, Am Mühlenberg 1, 14476 Golm, Germany*

(Dated: July 1, 2005)

We propose a generalization of the condition for harmonic spatial coordinates analogous to the generalization of the harmonic time slices introduced by Bona *et al.* These generalized harmonic spatial coordinates imply a condition for the shift vector that has the form of an evolution equation for the shift components. We find that in order to decouple the slicing condition from the evolution equation for the shift it is necessary to use a rescaled shift vector. We also analyze the effect of the shift condition proposed here on the hyperbolicity of the evolution equations of general relativity in 1+1 dimensions and 3+1 spherical symmetry, and study the possible development of blowups. Finally, we perform a series of numerical experiments to illustrate the behavior of this shift condition.

PACS numbers: 04.20.Ex, 04.25.Dm, 95.30.Sf

Preprint number: AEI-2005-108

## I. INTRODUCTION

When one studies the time evolution of the gravitational field in general relativity, a good choice of coordinates (a “gauge” choice) can make the difference between finding a well behaved solution for a large portion of the spacetime, or rapidly running into a coordinate (or physical) singularity. In the 3+1 formulation, the choice of the time coordinate is related with the lapse function, while the choice of the spatial coordinates is related to the shift vector. Many different ways to choose the lapse and the shift have been proposed and used in numerical simulations in the past (see for example the pioneering papers of Smarr and York [1, 2]). Some gauge choices involve solving elliptic equations, while others involve solving evolution type equations, which may or may not be hyperbolic in character. Recently, hyperbolic coordinate conditions have become a focus of attention, as they in principle allow one to write the full set of dynamical equations as a well-posed system [3, 4, 5, 6, 7, 8], while at the same time being both easier to implement and considerably less computationally expensive than elliptic conditions.

The classic example of hyperbolic coordinate conditions are the so-called harmonic coordinates, which are defined by asking for the wave operator acting on the coordinate functions  $x^\mu$  to vanish. Harmonic coordinate conditions have the important property of allowing the Einstein field equations to be written as a series of wave equations, with non-linear source terms, for the metric coefficients  $g_{\mu\nu}$ . Because of this, these conditions were used to prove the first theorems on the existence of solutions to the Einstein equations [9]. This property of transforming the Einstein equations into wave equations could in principle also be seen as an important advantage in the numerical integration of these equations. Still, with few exceptions (see for example [10, 11, 12]), full harmonic coordinates have traditionally not been used in numerical relativity, though harmonic time slices have been advocated and used in some cases [13, 14, 15, 16]. The reason for this is two-fold: In the first place, har-

monic coordinates are rather restrictive, and formulations of the Einstein equations for numerical relativity are usually written in a way that allows the gauge freedom to remain explicit so it can be used to control certain aspects of the evolution (avoid singularities, enforce symmetries, reduce shear, etc.). Also, in the particular case of a harmonic time coordinate, it has been shown that the space-like foliation avoids focusing singularities only marginally, and is therefore not a good choice in many cases [4, 13, 17, 18]. Of course, it can be argued that any coordinate choice is harmonic if one does not ask for the wave operator acting on the coordinate functions to vanish, but instead to be equal to an arbitrary function of spacetime (a “gauge source function”). This is certainly true, but of little use in real life numerical simulations where there is no way to know *a priori* what is a convenient choice for these gauge source functions (but see [12] for some suggestions that seem to work well in practice).

Nevertheless, the fact that the use of harmonic coordinates allows the field equations to be written in manifestly hyperbolic form makes one immediately ask if there might be simple generalizations of the harmonic conditions that will still allow the field equations to be written in hyperbolic form, while at the same time retaining a useful degree of gauge freedom. That this is indeed the case was first shown for the particular case of a harmonic time coordinate by Bona *et al.* in [19], where a hyperbolic reformulation of the Einstein evolution equations was constructed using a generalized harmonic slicing condition. This generalized harmonic slicing condition, usually referred to as the Bona-Masso slicing condition, includes as particular cases several choices that had been used in numerical simulations from the early 90’s with good results, such as for example the “1+log” slicing [20, 21]. In fact, the Bona-Masso slicing condition was motivated precisely to include such empirically tested conditions in a strongly hyperbolic formulation of the Einstein equations.

In this paper we want to follow a similar approach and propose a generalization of the harmonic spatial coor-

dinate condition. We will show how this allows us to obtain a hyperbolic shift condition that is similar to conditions already proposed in the literature, most notably the shift conditions recently introduced by Lindblom and Scheel [8] and by Bona and Palenzuela [22].

This paper is organized as follows. In Sec. II we discuss the standard harmonic coordinates and write them as evolution equations for the lapse and shift. We also introduce a rescaled shift vector that allows one to decouple the lapse and shift equations. Section III generalizes the condition of spatial harmonic coordinates. In Sec. IV we describe the concept of hyperbolicity and the source criteria for avoiding blowups. Section V studies the generalized harmonic shift condition in the case of 1+1 dimensions, analyzing its hyperbolicity properties, the possible appearance of blowups (gauge shocks), and also the behavior of this shift condition in numerical simulations. In Sec. VI we repeat the same type of analysis for spherical symmetry and also present results from numerical simulations. We conclude in Sec. VII. Finally, Appendix A shows a formal derivation of the generalized harmonic lapse and shift conditions, and Appendix B gives general expressions for the 4-Christoffel symbols in terms of 3+1 quantities.

## II. HARMONIC COORDINATES

Let us consider four scalar coordinate functions  $\phi^\alpha$  defined on a given background spacetime. The condition for these coordinates to be harmonic is simply

$$\square\phi^\alpha := g^{\mu\nu} \nabla_\mu \nabla_\nu \phi^\alpha = 0, \quad (2.1)$$

with  $g_{\mu\nu}$  the spacetime metric tensor.

Let us further assume that  $\phi^0$  is such that its level surfaces are space-like. In that case,  $\phi^0$  can be identified with a global time function. If we define the lapse function  $\alpha$  as the interval of proper time when going from the hypersurface  $\phi^0 = t$  to the hypersurface  $\phi^0 = t + dt$  along the normal direction, then it is easy to show that  $\alpha$  will be given in terms of  $\phi^0$  as

$$\alpha = (-\nabla\phi^0 \cdot \nabla\phi^0)^{-1/2}. \quad (2.2)$$

The definition of the shift vector is somewhat more involved. We start by defining three scalar functions  $\beta^a$  such that when we move from a given level surface of  $\phi^0$  to the next following the normal direction, the change in the spatial coordinate functions  $\phi^a$  is given by

$$\phi_{t+dt}^a = \phi_t^a - \beta^a d\phi^0, \quad (2.3)$$

from which one can easily find

$$\beta^a = -\alpha (\vec{n} \cdot \nabla\phi^a), \quad (2.4)$$

with  $\vec{n}$  the unit normal vector to the hypersurface  $\phi^0 = t$ ,

$$\vec{n} = -\alpha \nabla\phi^0, \quad (2.5)$$

and where the minus sign is there to guarantee that  $\vec{n}$  is future pointing. Thus defined, the  $\beta^a$  are scalars, but we can use them to define a vector  $\vec{\beta}$  by asking for its components in the coordinate system  $\{\phi^\alpha\}$  to be given by  $(0, \beta^a)$ . The vector constructed in this way is clearly orthogonal to  $\vec{n}$ . In an arbitrary coordinate system  $\{x^\mu\}$ , the shift components will then be given by

$$\beta^\mu = -\alpha (\vec{n} \cdot \nabla\phi^a) \frac{\partial x^\mu}{\partial\phi^a}. \quad (2.6)$$

Notice that with this definition, the shift vector is proportional to the lapse function, so that a simple rescaling of  $\phi^0$  changes the shift. This suggests that it is perhaps more natural to define a rescaled shift vector  $\vec{\sigma}$  in the following way

$$\sigma^\mu := \frac{\beta^\mu}{\alpha} = -(\vec{n} \cdot \nabla\phi^a) \frac{\partial x^\mu}{\partial\phi^a}. \quad (2.7)$$

We will see below that this rescaled shift vector will be important when expressing the harmonic condition in 3+1 language.

The harmonic coordinate conditions can be simplified by expanding them in the coordinate system  $\{x^\alpha = \phi^\alpha\}$ , in which case they reduce to

$$\Gamma^\alpha := g^{\mu\nu} \Gamma_{\mu\nu}^\alpha = 0, \quad (2.8)$$

where  $\Gamma_{\mu\nu}^\alpha$  are the Christoffel symbols associated with the 4-metric  $g_{\mu\nu}$ . If we now relate the coordinates  $\{x^\alpha = \phi^\alpha\}$  to the standard 3+1 coordinates, then these four equations can be shown to become (see Appendix A and B)

$$\partial_t \alpha = \beta^a \partial_a \alpha - \alpha^2 K, \quad (2.9)$$

$$\begin{aligned} \partial_t \beta^i &= \beta^a \partial_a \beta^i - \alpha \partial^i \alpha + \alpha^2 {}^{(3)}\Gamma^i \\ &+ \frac{\beta^i}{\alpha} (\partial_t \alpha - \beta^a \partial_a \alpha + \alpha^2 K). \end{aligned} \quad (2.10)$$

Here  $K$  is the trace of the extrinsic curvature, and  ${}^{(3)}\Gamma^i$  is defined in terms of the three-dimensional Christoffel symbols  ${}^{(3)}\Gamma_{jk}^i$ , the spatial metric  $\gamma_{ij}$  and its determinant  $\gamma := \det \gamma_{ij}$  by  ${}^{(3)}\Gamma^i := \gamma^{jk} {}^{(3)}\Gamma_{jk}^i = -\partial_j (\sqrt{\gamma} \gamma^{ij}) / \sqrt{\gamma}$ . Notice that in equation (2.10) we have an explicit dependency on the time derivative of the lapse function. This dependency is usually not written down, as the whole last term of the second equation vanishes if the first equation is assumed to hold, but we prefer to leave the dependency explicit (see for example [11, 23]; incidentally, equation (2.10) fixes a sign error in [23], and includes a term missing in [11]).

The fact that the evolution equation for the shift depends on the time derivative of the lapse is inconvenient if one wants to use harmonic spatial coordinates with a different slicing condition, say maximal slicing. It is also an indication that the shift itself might not be the most convenient function to evolve. Remarkably, it turns out that if we rewrite the evolution equation for the shift in terms of the rescaled shift  $\sigma^i = \beta^i / \alpha$  introduced above,

then the spatial harmonic condition decouples completely from the evolution of the lapse. We find

$$\partial_t \sigma^i = \alpha \sigma^a \partial_a \sigma^i - \partial^i \alpha + \alpha \left( \sigma^i K + {}^{(3)}\Gamma^i \right) . \quad (2.11)$$

Therefore, if one works with  $\sigma^i$  instead of  $\beta^i$ , one can use harmonic spatial coordinates with an arbitrary slicing condition in a straightforward way.

A final comment about equations (2.9) and (2.10) is in order. Equation (2.9) is clearly a scalar equation as seen in the spatial hypersurfaces. Equation (2.10), on the other hand, is not 3-covariant, *i.e.* starting from exactly the same 3-geometry but in different coordinates, it will produce a different evolution for the shift vector. This might seem surprising since this equation is just the 3+1 version of the condition for spatial harmonic coordinates which is 4-covariant. However, there is no real contradiction, since changing the coordinates on the spatial hypersurfaces means changing the scalar functions  $\phi^i$  themselves, so it should not be surprising that we get a different shift.

### III. GENERALIZED HARMONIC COORDINATES

In [19], Bona *et al.* generalize the harmonic slicing condition (2.9) in the following way

$$\partial_t \alpha - \beta^a \partial_a \alpha = -\alpha^2 f(\alpha) K , \quad (3.1)$$

with  $f(\alpha)$  a positive but otherwise arbitrary function of the lapse. This slicing condition was originally motivated by the Bona-Masso hyperbolic reformulation of the Einstein equations [14, 15, 17, 19, 24], but can in fact be used with any form of the 3+1 evolution equations. As shown in [4], the Bona-Masso slicing condition above can be shown to avoid both focusing singularities [17] and gauge shocks [25] for particular choices of  $f$ . Reference [4] also shows that condition (3.1) can be written in 4-covariant form in terms of a global time function  $\phi^0$  as

$$(g^{\mu\nu} - a_f n^\mu n^\nu) \nabla_\mu \nabla_\nu \phi^0 = 0 , \quad (3.2)$$

with  $a_f := 1/f(\alpha) - 1$  and  $n^\mu$  the unit normal vector to the spatial hypersurfaces defined in (2.5). Here we will introduce an analogous generalization of the spatial harmonic coordinates  $\{\phi^i\}$ . That is, we propose the following spatial gauge condition

$$(g^{\mu\nu} - a_h n^\mu n^\nu) \nabla_\mu \nabla_\nu \phi^l = 0 , \quad (3.3)$$

where  $n^\mu$  is still the unit normal to the spatial hypersurfaces, but now  $a_h := 1/h - 1$ , with  $h(\alpha, \beta^i)$  a scalar function that can in principle depend on both the lapse and shift (we will see below that the shift dependence is in fact not convenient). In the coordinate system  $\{x^\mu = \phi^\mu\}$ , condition (3.3) becomes

$$(g^{\mu\nu} - a_h n^\mu n^\nu) \Gamma_{\mu\nu}^l = 0 . \quad (3.4)$$

Expressing the 4-metric and normal vector in terms of 3+1 variables, the last equation becomes

$$\Gamma_{00}^l - 2\beta^m \Gamma_{m0}^l + \beta^m \beta^n \Gamma_{mn}^l = \alpha^2 h \gamma^{mn} \Gamma_{mn}^l . \quad (3.5)$$

Notice that on the right hand side of this equation appears the contraction  $\gamma^{mn} \Gamma_{mn}^l$  which should not be confused with  $\Gamma^l := g^{\mu\nu} \Gamma_{\mu\nu}^l$ . Inserting now the expressions for the  $\Gamma_{mn}^l$  found in Appendix B we obtain

$$\begin{aligned} \partial_t \beta^l &= \beta^m \partial_m \beta^l - \alpha \partial^l \alpha + \frac{\beta^l}{\alpha} (\partial_t \alpha - \beta^m \partial_m \alpha) \\ &+ \alpha^2 h \left( \frac{\beta^l}{\alpha} K + {}^{(3)}\Gamma^l \right) . \end{aligned} \quad (3.6)$$

This is to be compared with equation (2.10) of the previous section. Notice that again we find that the evolution equation for the shift is coupled to that of the lapse. In the same way as before, we can decouple the shift evolution equation by writing it in terms of the rescaled shift  $\sigma^i = \beta^i/\alpha$ . We find

$$\partial_t \sigma^l = \alpha \sigma^m \partial_m \sigma^l - \partial^l \alpha + \alpha h \left( \sigma^l K + {}^{(3)}\Gamma^l \right) , \quad (3.7)$$

which is to be compared with (2.11). This is the final form of the condition for generalized harmonic spatial coordinates, and we will refer to this condition simply as the “generalized harmonic shift”.

In the following sections we will study this shift condition. We will first introduce in Sec. IV the concept of hyperbolicity, and a criteria for avoiding blowups in the solutions of hyperbolic systems of equations. Later, in Sections V and VI we will consider the special cases of 1+1 dimensional relativity and spherical symmetry. In each case we will analyze the hyperbolicity properties of the full system of equations *including* the generalized harmonic shift condition, study the possible development of blowups (gauge shocks), and present a series of numerical examples.

## IV. HYPERBOLICITY AND SHOCKS

### A. Hyperbolic systems

The concept of hyperbolicity is of fundamental importance in the study of the evolution equations associated with a Cauchy problem. Intuitively, hyperbolicity is related to causality in the sense that the solution at a given point in spacetime depends only on data in a region of compact support to the past of that point. Furthermore, strongly or symmetric hyperbolic systems can be shown to be well-posed (though the well-posedness of strongly hyperbolic systems requires that some additional smoothness conditions are verified). In the following we will concentrate on one-dimensional systems, for which the distinction between strongly and symmetric hyperbolic systems does not arise.

We will consider quasi-linear systems of evolution equations that can be split into two subsystems with the following structure

$$\partial_t \vec{u} = \mathbf{M}(\vec{u}) \vec{v}, \quad (4.1)$$

$$\partial_t \vec{v} + \mathbf{A}(\vec{u}) \partial_x \vec{v} = \vec{q}_v(\vec{u}, \vec{v}), \quad (4.2)$$

where  $\vec{u}$  and  $\vec{v}$  are  $n$  and  $m$  dimensional vectors, and where  $\mathbf{M}$  and  $\mathbf{A}$  are  $n \times n$  and  $m \times m$  matrices, respectively. In addition we demand that the  $v$ 's are related to either time or space derivatives of the  $u$ 's. This implies that derivatives of the  $u$ 's can always be substituted for  $v$ 's and hence treated as source terms. In our primary example, the Einstein equations, the vector  $\vec{u}$  consists of gauge variables and components of the 3-metric, whereas  $\vec{v}$  contains both variables associated with the spatial derivatives of the gauge variables and metric components and also extrinsic curvature components. Note, furthermore, that the source terms  $\vec{q}_v$  appearing on the right hand side of (4.2) are in general functions of both the  $u$ 's and  $v$ 's (typically quadratic on the  $v$ 's).

The system of equations above will be hyperbolic if the matrix  $\mathbf{A}$  has  $m$  real eigenvalues  $\lambda_i$ . Furthermore, it will be strongly hyperbolic if it has a complete set of eigenvectors  $\vec{\xi}_i$ ,

$$\mathbf{A} \vec{\xi}_i = \lambda_i \vec{\xi}_i. \quad (4.3)$$

If we denote the matrix of column eigenvectors by  $\mathbf{R}$ ,

$$\mathbf{R} = \left( \vec{\xi}_1 \cdots \vec{\xi}_m \right), \quad (4.4)$$

then the matrix  $\mathbf{A}$  can be diagonalized as

$$\mathbf{R}^{-1} \mathbf{A} \mathbf{R} = \text{diag} [\lambda_1, \dots, \lambda_m] = \mathbf{\Lambda}. \quad (4.5)$$

For a strongly hyperbolic system we then define the eigenfields as

$$\vec{w} = \mathbf{R}^{-1} \vec{v}. \quad (4.6)$$

By analyzing the time evolution of the eigenfields, one can identify mechanisms that lead to blowups in the solution, which in [26] have been referred to as “geometric blowup” and the “ODE-mechanism”. Since in the first case the derivative of an evolution variable, and in the second case an evolution variable itself, becomes infinite within a finite time, the names “gradient catastrophe” [27] and “blowup within finite time” are probably more appropriate here. In [28] some of us presented blowup avoiding conditions for both these mechanisms, which we called “indirect linear degeneracy” [25] and the “source criteria”. In that reference it was also shown, using numerical examples, that the source criteria for avoiding blowups is generally the more important of the two conditions. Because of this, and also because of the fact that the true relevance of indirect linear degeneracy is not as yet completely clear, in this paper we will concentrate only on the source criteria.

## B. Source criteria for avoiding blowups

An evolution variable can become infinite at a given point by a process of “self-increase” in the causal past of this point. The underlying mechanism has been given the name “ODE-mechanism” [26], since prototype examples are based on simple ordinary differential equations (ODE's) such as  $du/dt = cu^2$ , where  $c = \text{const} \neq 0$ . For non-trivial initial data the solution of this equation is given by  $u(t) = u_0/(1 - u_0 ct)$ , which clearly blows up at a finite time  $t^* = 1/u_0 c$  (which will be in the past or in the future depending on the sign of  $u_0 c$ ).

A criteria to avoid such blowups for systems of partial differential equations (PDE's) of the form (4.1) - (4.2) was proposed by some of us in [28]. When diagonalizing the evolution system for the  $v$ 's, making use of (4.5) and (4.6), one finds

$$\partial_t \vec{w} + \mathbf{\Lambda} \partial_x \vec{w} = \vec{q}_w, \quad (4.7)$$

where

$$\vec{q}_w := \mathbf{R}^{-1} \vec{q}_v + [\partial_t \mathbf{R}^{-1} + \mathbf{\Lambda} \partial_x \mathbf{R}^{-1}] \vec{v}. \quad (4.8)$$

This gives us an evolution system where on the left-hand side of (4.7) the different eigenfields  $w_i$  are decoupled. However, in general the equations are still coupled through the source terms  $q_{w_i}$ . In particular, if the original sources were quadratic in the  $v$ 's, one obtains

$$\frac{dw_i}{dt} = \partial_t w_i + \lambda_i \partial_x w_i = \sum_{j,k=1}^m c_{ijk} w_j w_k + \mathcal{O}(w), \quad (4.9)$$

where  $d/dt := \partial_t + \lambda_i \partial_x$  denotes the derivative along the corresponding characteristic. As pointed out in [28], the  $c_{iii} w_i^2$  component of the source term can be expected to dominate, so that the mixed and lower order terms can be neglected. In this case one can then rewrite the above equation as

$$\frac{dw_i}{dt} \approx c_{iii} w_i^2, \quad (4.10)$$

which has precisely the form of the ODE mentioned earlier in this section. In order to avoid possible blowups of the solutions we therefore demand that the coefficients  $c_{iii}$  should vanish. We call this condition the “source criteria” for avoiding blowups.

Though no general proof of the fact that the source criteria is a necessary condition for avoiding blowups has been presented in [28], one can expect it to be true at least for small perturbations propagating with distinct eigenspeeds, as mixed terms will then be suppressed when pulses moving at different speeds separate from each other. The effect of the term  $c_{iii} w_i^2$ , on the other hand, will remain as the pulse moves. If, however, some eigenfields  $w_i$  and  $w_j$  travel with identical or similar eigenspeeds, then one should also expect important contributions coming from the mixed terms  $w_i w_j$ . We will show

an example later on where eliminating such mixed terms (in addition to the quadratic terms) indeed leads to further improvements.

Two very important properties of our system of equations regarding the coefficients  $c_{iii}$  were pointed out in [28] (these properties hold as long as the constraints relating some of the  $v$ 's with spatial derivatives of the  $u$ 's remain satisfied): In the first place, from (4.8) one could expect contributions to the coefficients  $c_{iii}$  coming both from the original sources  $\vec{q}_v$  and from the term in brackets involving derivatives of  $\mathbf{R}^{-1}$ . However, one can show that this is not the case and for the systems under study the contributions to  $c_{iii}$  coming from the term in brackets cancel out, that is, all contributions to  $c_{iii}$  come only from the original sources  $\vec{q}_v$ . Furthermore, as the eigenvectors  $\vec{\xi}_i$  diagonalizing the matrix  $\mathbf{A}$  are obtained only up to an arbitrary rescaling, the eigenfields  $w_i$  are in fact not unique. In particular, any  $w_i$  can be multiplied by an arbitrary function of the  $u$ 's to obtain  $\tilde{w}_i = \Omega_i(\vec{u}) w_i$ . Remarkably, for the systems of the type (4.1)-(4.2) that we are interested in, it turns out that such rescalings of the eigenfields have also no effect on the coefficients  $c_{iii}$ .

## V. EINSTEIN EQUATIONS IN 1+1 DIMENSIONS

Let us assume that we have standard general relativity in one spatial dimension and in vacuum. It is well known that in such a case the gravitational field is trivial and there are no true dynamics. However, one can still have non-trivial evolutions due to gauge dynamics that can be used as a simple example of the type of behavior one can expect in the higher dimensional case. Since in this paper we are interested precisely in studying a new shift condition, 1+1 dimensional relativity is an ideal initial testing ground.

In the following sections we will introduce the evolution equations and gauge conditions, and consider the possible formation of blowups associated with our gauge conditions. We will also present numerical simulations that show how the generalized harmonic shift condition behaves in practice.

### A. Evolution equations

We will start from the “standard” Arnowitt-Deser-Misner (ADM) equations for one spatial dimension [29], where by standard we mean the version of York [23]. In this case the three-dimensional vector  $\vec{u}$  consists of the lapse function  $\alpha$ , the rescaled shift  $\sigma := \sigma^x$  and the spatial metric function  $g := g_{xx}$ . The vector  $\vec{v}$ , on the other hand, is a four-dimensional vector with components given by the spatial derivatives of the  $u$ 's and, in addition, the unique component of the extrinsic curvature. That is,

$$\vec{u} = (\alpha, \sigma, g) , \quad \vec{v} = (D_\alpha, d_\sigma, D_g, \tilde{K}) , \quad (5.1)$$

with  $\tilde{K} := \sqrt{g} \operatorname{tr} K = \sqrt{g} K_x^x$ , and where we have defined

$$D_\alpha := \partial_x \ln \alpha , \quad D_g := \partial_x \ln g , \quad d_\sigma := \partial_x \sigma . \quad (5.2)$$

Notice first that we use a rescaled extrinsic curvature, as this makes the evolution equations considerably simpler. Also, we use logarithmic spatial derivatives of  $\alpha$  and  $g$ , but only the ordinary spatial derivative of the rescaled shift  $\sigma$ , as the shift is allowed to change sign.

For the evolution of the gauge variables we will use the Bona-Masso slicing condition (3.1) and the generalized harmonic shift condition (3.7). The equations for the  $u$ 's are then

$$\partial_t \alpha = \alpha^2 \left[ \sigma D_\alpha - \frac{f \tilde{K}}{\sqrt{g}} \right] , \quad (5.3)$$

$$\partial_t \sigma = \alpha \left[ \sigma d_\sigma - \frac{D_\alpha}{g} + h \left( \frac{D_g}{2g} + \frac{\sigma \tilde{K}}{\sqrt{g}} \right) \right] , \quad (5.4)$$

$$\partial_t g = \alpha g \left[ \sigma D_g + 2 \left( d_\sigma + \sigma D_\alpha - \frac{\tilde{K}}{\sqrt{g}} \right) \right] , \quad (5.5)$$

where  $f = f(\alpha)$  and  $h = h(\alpha, \sigma)$ . The evolution equations for  $\{D_\alpha, d_\sigma, D_g\}$  can be obtained directly from the above equations, while the evolution equation for  $\tilde{K}$  comes from the ADM equations and takes the following simple form

$$\partial_t \tilde{K} = \partial_x \left[ \alpha \left( \sigma \tilde{K} - D_\alpha / \sqrt{g} \right) \right] . \quad (5.6)$$

The Einstein equations for the vector  $\vec{v}$  can then be written in full conservative form  $\partial_t \vec{v} + \partial_x (\mathbf{A} \vec{v}) = 0$ , with the characteristic matrix  $\mathbf{A}$  given by

$$\mathbf{A} = \begin{pmatrix} -\alpha\sigma & 0 & 0 & \alpha f / \sqrt{g} \\ \alpha/g & -\alpha\sigma & -\alpha h/2g & -\alpha h\sigma / \sqrt{g} \\ -2\alpha\sigma & -2\alpha & -\alpha\sigma & 2\alpha / \sqrt{g} \\ \alpha / \sqrt{g} & 0 & 0 & -\alpha\sigma \end{pmatrix} . \quad (5.7)$$

This matrix has the following eigenvalues

$$\lambda_\pm^f = \alpha \left( \pm \sqrt{f/g} - \sigma \right) , \quad (5.8)$$

$$\lambda_\pm^h = \alpha \left( \pm \sqrt{h/g} - \sigma \right) , \quad (5.9)$$

with corresponding eigenfunctions (the normalization is chosen for convenience)

$$w_\pm^f = \tilde{K} \pm D_\alpha / \sqrt{f} , \quad (5.10)$$

$$w_\pm^h = - \left( 1 \pm \sigma \sqrt{gh} \right) \tilde{K} + \sqrt{g} d_\sigma \mp \sqrt{h} D_g / 2 , \quad (5.11)$$

which can be easily inverted to find

$$D_\alpha = \frac{\sqrt{f}}{2} (w_+^f - w_-^f) , \quad (5.12)$$

$$d_\sigma = \frac{1}{2\sqrt{g}} (w_+^f + w_-^f + w_+^h + w_-^h) , \quad (5.13)$$

$$D_g = \frac{1}{\sqrt{h}} (w_-^h - w_+^h) - \sigma \sqrt{g} (w_+^f + w_-^f) , \quad (5.14)$$

$$\tilde{K} = \frac{1}{2} (w_+^f + w_-^f) . \quad (5.15)$$

The system is therefore strongly hyperbolic as long as  $f > 0$  and  $h > 0$ , with the lapse and shift eigenfields  $w_\pm^f$  and  $w_\pm^h$  propagating with the corresponding gauge speeds  $\lambda_\pm^f$  and  $\lambda_\pm^h$ .

### B. Gauge shock analysis

By analyzing quadratic source terms in the evolution equations of the eigenfields  $w_i$ , we now want to study the possible formation of blowups for the system of evolution equations of the previous section. For the lapse and shift eigenfields we find

$$\begin{aligned} \frac{dw_\pm^f}{dt} &= c_{\pm\pm\pm}^{fff} w_\pm^{f2} + c_{\pm\pm\pm}^{ffh} w_\pm^f w_\pm^h \\ &+ \mathcal{O}(w_\pm^f w_\mp^f, w_\pm^h w_\mp^h) , \end{aligned} \quad (5.16)$$

$$\begin{aligned} \frac{dw_\pm^h}{dt} &= c_{\pm\pm\pm}^{hhh} w_\pm^{h2} + c_{\pm\pm\pm}^{hhf} w_\pm^h w_\pm^f \\ &+ \mathcal{O}(w_\pm^h w_\mp^h, w_\pm^f w_\mp^f) . \end{aligned} \quad (5.17)$$

In particular, we observe that in (5.16) no term proportional to  $w_\pm^{h2}$  is present, and in the same way in (5.17) there is no term proportional to  $w_\pm^{f2}$ . In order to apply the source criteria we need to calculate those terms quadratic in  $w_i$  appearing in the sources of the evolution equation for  $w_i$  itself. It turns out that the  $c_{iii}$  coefficients have the form

$$c_{\pm\pm\pm}^{fff} \propto (1 - f - \alpha f'/2) , \quad (5.18)$$

$$c_{\pm\pm\pm}^{hhh} \propto \partial h / \partial \sigma . \quad (5.19)$$

According to the source criteria these coefficients have to vanish in order to avoid blowups. The conditions on the gauge functions  $f(\alpha)$  and  $h(\alpha, \sigma)$  are then

$$1 - f - \alpha f'/2 = 0 , \quad (5.20)$$

$$\partial h / \partial \sigma = 0 . \quad (5.21)$$

The condition (5.20) for  $f(\alpha)$  has been studied many times before [4, 25, 28, 30], and its general solution is

$$f(\alpha) = 1 + \text{const}/\alpha^2 . \quad (5.22)$$

For  $h(\alpha, \sigma)$ , on the other hand, we obtain the condition that  $h$  can be an (arbitrary) function of  $\alpha$ , but may not depend on  $\sigma$ , that is,  $h = h(\alpha)$ .

One now might wonder about the case where  $h$  is equal (or very close to) the function  $f$ . In that case the eigenfields  $w_\pm^f$  and  $w_\pm^h$  travel with the same (or similar) eigenspeeds, so mixed terms of the type  $w_\pm^f w_\pm^h$  in the sources can be expected to contribute to a blowup. For this reason we have also calculated the  $c_{iij}$  coefficients associated to these terms. Notice, however, that in general the coefficients of such mixed terms are not invariant under rescalings of the eigenfields of the form  $\tilde{w}_i = \Omega_i(\alpha, \sigma, g) w_i$ , so we have in fact done the calculation assuming an arbitrary rescaling. We find

$$c_{\pm\pm\pm}^{ffh} \propto \left( 1 - \sqrt{\frac{h}{f}} \right) , \quad (5.23)$$

$$\begin{aligned} c_{\pm\pm\pm}^{hhf} &\propto \left\{ \left[ 2\alpha \sqrt{f} \frac{\partial \Omega_\pm^h}{\partial \alpha} \pm \frac{2}{\sqrt{g}} \frac{\partial \Omega_\pm^h}{\partial \sigma} \right. \right. \\ &\mp 4\sigma \sqrt{g} \left( \Omega_\pm^h + g \frac{\partial \Omega_\pm^h}{\partial g} \right) \left. \right] \left( 1 - \sqrt{\frac{h}{f}} \right) \\ &+ \left[ \frac{\sqrt{f}}{2h} \left( 1 + \sqrt{\frac{h}{f}} \right) \left( \alpha \frac{\partial h}{\partial \alpha} \pm \frac{1}{\sqrt{g}f} \frac{\partial h}{\partial \sigma} \right) \right. \\ &\left. \left. + \frac{1+3h}{\sqrt{h}} - \frac{3+h}{\sqrt{f}} \right] \Omega_\pm^h \right\} . \end{aligned} \quad (5.24)$$

One can readily verify that these coefficients vanish for  $f = h = 1 + \text{const}/\alpha^2$ , independently of the rescaling of the eigenfields. This setting of  $f$  and  $h$  hence seems to be an optimal choice for avoiding blowups.

### C. Numerical examples

In order to test the generalized harmonic shift condition we have performed a series of numerical experiments. We evolve Minkowski initial data, but with a non-trivial initial slice given in Minkowski coordinates  $(t_M, x_M)$  as  $t_M = p(x_M)$ , with  $p$  a profile function that decays rapidly. If we use  $x = x_M$  as our spatial coordinate, the spatial metric and extrinsic curvature turn out to be

$$g(t=0) = 1 - p'^2 , \quad \tilde{K}(t=0) = -p''/g . \quad (5.25)$$

In all the simulations shown below we have taken for the function  $p(x)$  a Gaussian centered at the origin

$$p(x) = \kappa \exp \left[ - \left( \frac{x}{s} \right)^2 \right] . \quad (5.26)$$

For our simulations we have chosen for  $\kappa$  and  $s$  the same values used in [25], namely  $\kappa = 5$  and  $s = 10$ . Furthermore, we start with unit lapse and vanishing shift.

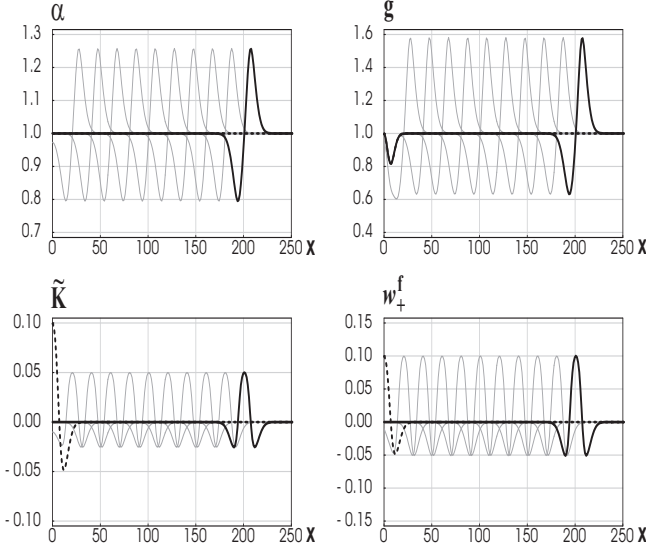


FIG. 1: For a simulation with harmonic slicing ( $f = 1$ ) and vanishing shift, we show the evolution in time of the variables  $\alpha$ ,  $g$  and  $\tilde{K}$ , together with that of the eigenfield  $w_+^f$ . The values of the different quantities are shown every  $\Delta t = 20$ .

All runs have been performed using a method of lines with fourth order Runge-Kutta integration in time, and standard second order centered differences in space. Furthermore, we have used 16,000 grid points and a grid spacing of  $\Delta x = 0.05$  (which places the boundaries at  $\pm 400$ ), together with a time step of  $\Delta x/4$ . In the simulations shown below, we will concentrate on two different aspects: First, we want to know how the generalized harmonic shift condition works in practice, and what are its effects on the evolution. Also, we want to see if gauge shocks do form when they are expected.

The first run shown in Fig. 1 corresponds to harmonic slicing and vanishing shift (these plots should be compared with Fig. 2 of [25]). In the figures, the initial data is shown as a dashed line, and the final values at  $t = 200$  as a solid line. Intermediate values at intervals of  $\Delta t = 20$  are shown in light gray. As can be seen from the plots, all variables behave in a wavelike fashion, with pulses moving out symmetrically in both directions away from the origin (we only show the  $x > 0$  side). A non-trivial distortion remains in  $g$ , indicating that even though at the end we return to trivial Minkowski slices, we are left with non-trivial spatial coordinates.

Our second example is shown in Fig. 2 and corresponds to  $f = h = 1$ , that is, pure harmonic coordinates in both space and time. The simulation is very similar to the previous one, except for the fact that now we have a non-trivial shift. The important thing to notice is that in this case the shift behaves in such a way that at the end of the run no distortion remains in the metric component  $g$  at the origin. This example allows us to understand the main effect that the introduction of the generalized harmonic shift has on the evolution: It drives the spatial coordinates to a situation where no final dis-

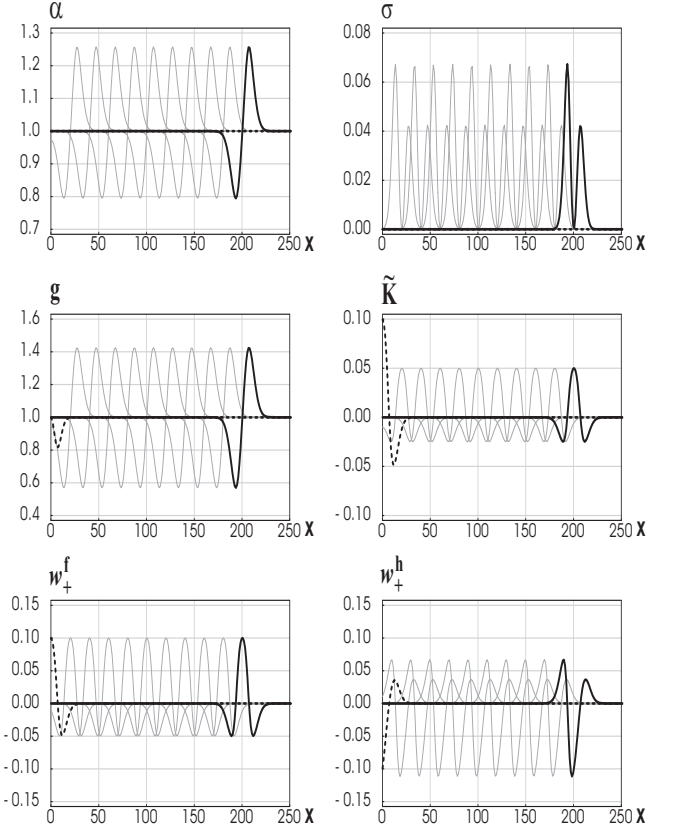


FIG. 2: For a simulation with harmonic slicing and harmonic shift ( $f = h = 1$ ), we show the evolution in time of  $\alpha$ ,  $\sigma$ ,  $g$  and  $\tilde{K}$ , together with that of  $w_+^f$  and  $w_+^h$ .

tortion in the metric is present. One should also note that for  $f = h = 1$  both eigenfields propagate with the same speed. However, since quadratic and mixed source terms in the evolution equations of both  $w_+^f$  and  $w_+^h$  are not present, simple wavelike behavior for all variables is observed.

A third example is presented in Fig. 3, which uses again  $f = 1$ , but now we take  $h = 1 + 3\sigma^2$ . Initially, the evolution behaves in a very similar way to the previous case. At later times, however, we observe that a sharp gradient develops in the rescaled shift  $\sigma$ , with a corresponding large spike in the shift eigenfield  $w_+^h$ . This causes the simulation to crash shortly after reaching the time  $t = 200$ . Such a blowup in  $w_+^h$  is expected in this case since the source criteria is not satisfied for  $h$  being a function of  $\sigma$ .

Our final example uses  $f = 1$  and  $h = 2$ , and is shown in Fig. 4. This example is interesting as the speeds for the lapse and shift eigenfields are different. Concentrate first on the evolution of the lapse, the extrinsic curvature and  $w_+^f$ . Here the evolution is essentially identical to that of the previous examples: A pulse travels with roughly unit speed, and behind it everything rapidly relaxes back to trivial values. The eigenfield  $w_+^h$ , on the other hand, shows a pulse traveling faster, with a speed  $\sim \sqrt{2}$ . It also takes considerably longer for the region behind this

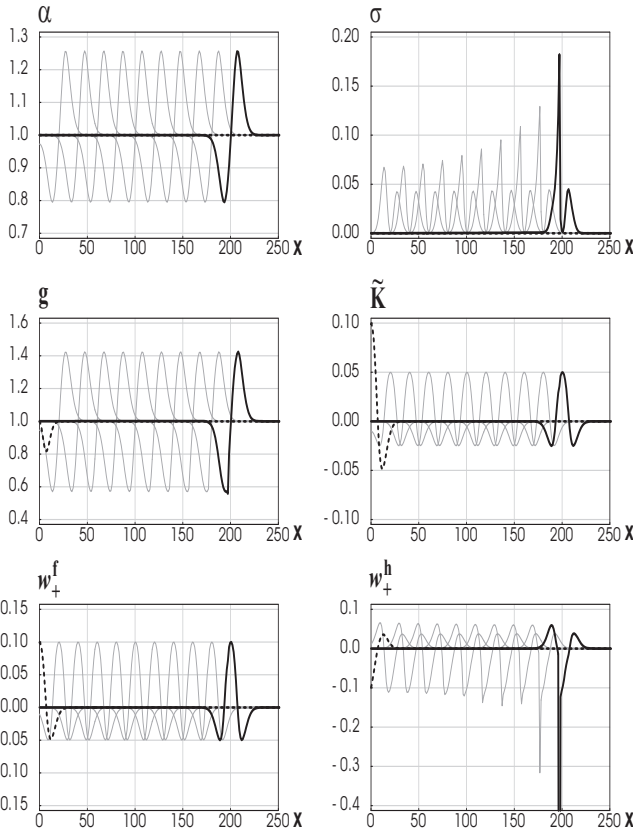


FIG. 3: For  $f = 1$  and  $h = 1 + 3\sigma^2$ , the simulation fails shortly after the time  $t = 200$  due to a sharp gradient developing in the rescaled shift  $\sigma$ , and a corresponding large spike appearing in the eigenfield  $w_{\pm}^h$ . This type of behavior is expected in this case since the source criteria is not satisfied.

pulse to relax to trivial values. Finally, the metric  $g$  and rescaled shift  $\sigma$  separate into two pulses traveling at the two different eigenspeeds. This is to be expected, as from (5.13) and (5.14) we see that metric and shift have contributions from both types of eigenfields.

To study the overall growth in the evolution variables, we introduce the quantity  $\delta$  defined through

$$\delta^2 := (\alpha - 1)^2 + \sigma^2 + (g - 1)^2 + \sum_{i=1}^4 v_i^2, \quad (5.27)$$

as a measure of how non-trivial the data is. For the different runs we study the behavior of the logarithm of the root mean square (rms) of  $\delta$  over time. In addition, since the behavior of the evolution turns out to depend to some extend on the initial data, and in particular on the sign of the Gaussian in (5.26), we perform runs for both  $\kappa = 5$  and  $\kappa = -5$ , and then take the average of both runs when calculating  $\delta$ . For the initial data we are using, at time  $t = 0$  this yields a value  $\log(\delta) \approx -1.583$  for both signs of  $\kappa$ .

In Fig. 5 we plot the rms of the quantity  $\delta$  for the times  $t = \{20, 40, 60, 80, 100\}$ , when using either  $h = 1$  and varying the (constant) value of  $f$  (top panel), or us-

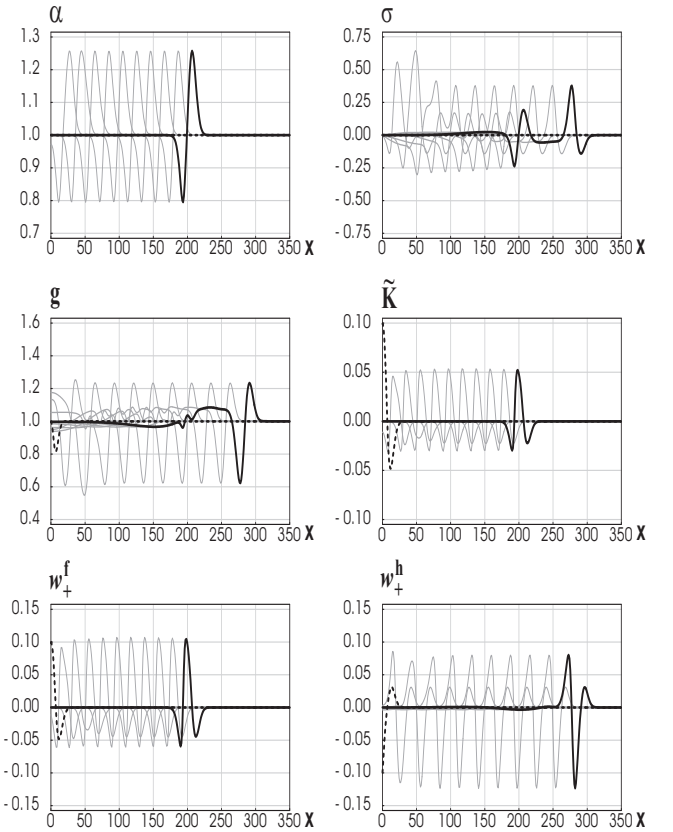


FIG. 4: For  $f = 1$  and  $h = 2$ , the lapse and shift eigenfields travel at different speeds. The lapse, extrinsic curvature and eigenfield  $w_{\pm}^f$  show a pulse traveling with roughly unit speed, while the eigenfield  $w_{\pm}^h$  shows a pulse moving with speed  $\sim \sqrt{2}$ . The metric  $g$  and rescaled shift  $\sigma$ , on the other hand, separate into two pulses traveling at the two different eigenspeeds.

ing  $f = 1$  together with different (again constant) values of  $h$  (bottom panel). From the top panel we see that  $f = 1$  is clearly preferred. In addition we want to point out that runs with  $f < 0.79$  and  $f > 1.25$  crashed before reaching the time  $t = 100$ . This behavior is expected as we know that constant values of  $f$  different from one produce blowups. In the lower panel we observe that for  $f = 1$  corresponding to harmonic slicing,  $h = 1$  performs best. In addition, values  $h \sim 0.5$  and  $h \gg 1$  also seem to be preferred. One should note that mixed terms  $w_{\pm}^f w_{\pm}^h$  in the evolution equations of both  $w_{\pm}^f$  and  $w_{\pm}^h$  for these choices of  $h$  play a minor role since localized perturbations in these eigenfields separate quickly when traveling with different speeds. We also want to mention that for  $h < 0.19$  the simulations again crashed before reaching the time  $t = 100$ . The observation that  $\delta$  grows rapidly and runs crash early if  $f$  and/or  $h$  are close to zero, can be understood by the fact that the system is not strongly hyperbolic for  $f = 0$  and/or  $h = 0$ .

In the contour plot of Fig. 6 we show the rms of  $\delta$  at time  $t = 100$  as a function of the gauge parameters  $f$  and

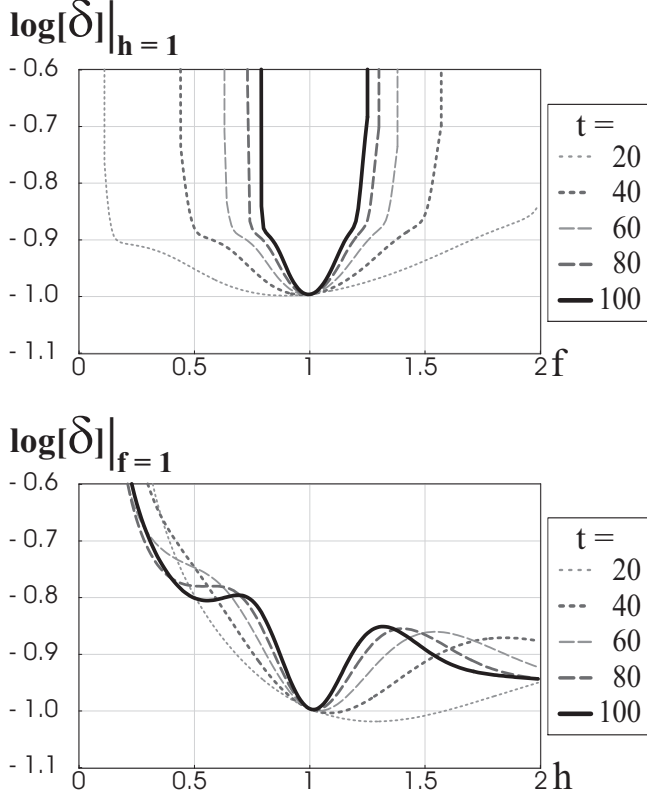


FIG. 5: *Top*. For evolutions with  $h = 1$ , the rms of  $\delta$  is shown on a logarithmic scale as a function of  $f$  every  $\Delta t = 20$ . The value  $f = 1$  is obviously preferred. *Bottom*. For runs with harmonic slicing ( $f = 1$ ), the same quantity is plotted as a function of  $h$ . Here  $h = 1$  is the optimal, and  $h \sim 0.5$  or  $h \gg 1$  are preferred choices.

$h$ , using  $64 \times 80$  equidistant parameter choices. Cases that have already crashed by that time correspond to the hashed regions. Note that the darker regions in this plot denote parameter choices where a significant growth in the evolution variables is present, and finally brighter regions correspond to runs with very little growth. We find small values for the rms of  $\delta$  for  $f$  being close to its shock avoiding value  $f = 1$ , and either  $h = 1$  or  $h \gg 1$ . In addition, we can also observe that  $f = h$  corresponds to a preferred choice. This can be explained by the fact that for this gauge choice the mixed terms  $w_{\pm}^f w_{\pm}^h$  are missing in the evolution equations of both  $w_{\pm}^f$  and  $w_{\pm}^h$ .

## VI. EINSTEIN EQUATIONS IN SPHERICAL SYMMETRY

As a second application of the generalized harmonic shift condition we will consider vacuum general relativity in spherical symmetry. This situation is considerably richer than the 1+1 dimensional case, but it also presents some special problems because of the singular nature of spherical coordinates at the origin.

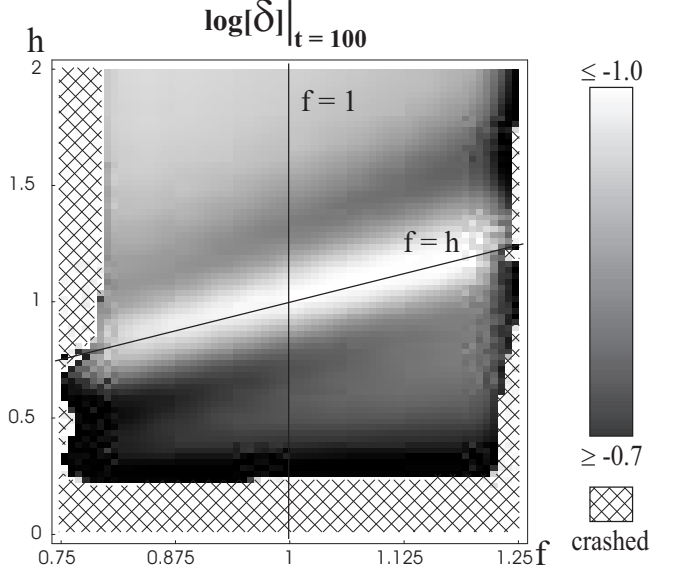


FIG. 6: Contour plot of the rms of  $\delta$  at time  $t = 100$ . Small values for this quantity are found for  $f = 1$ , when  $h = 1$  or  $h \gg 1$ , and for  $f = h$ .

### A. ADM evolution equations

We will consider the spherically symmetric line element written in the form

$$ds^2 = -\alpha^2 (1 - A\sigma^2) dt^2 + 2\alpha A\sigma dr dt + Adr^2 + Br^2 d\Omega^2, \quad (6.1)$$

where all the metric coefficients are functions of both  $t$  and  $r$ . We now introduce the following auxiliary variables

$$D_{\alpha} := \partial_r \ln \alpha, \quad d_{\sigma} := \partial_r \sigma, \quad (6.2)$$

$$D_A := \partial_r \ln A, \quad D_B := \partial_r \ln B. \quad (6.3)$$

Notice again that we use logarithmic derivatives for the lapse and the spatial metric, but only an ordinary derivative for the shift. For the extrinsic curvature, we will use the mixed components

$$K_A := K_r^r, \quad K_B := K_{\theta}^{\theta} = K_{\phi}^{\phi}. \quad (6.4)$$

Following [31], we will change our main evolution variables and make use of the “anti-trace” of the metric spatial derivatives  $D = D_A - 2D_B$ , and the trace of the extrinsic curvature  $K = K_A + 2K_B$ , instead of  $D_A$  and  $K_A$ .

For the regularization of the evolution equations at the origin we will follow the procedure described in [31], which requires the introduction of an auxiliary variable  $\lambda = (1 - A/B)/r$ . By taking  $\{\alpha, A, B, d_{\sigma}, K, K_B\}$  as even functions at  $r = 0$ , and  $\{\sigma, D_{\alpha}, D, D_B, \lambda\}$  as odd, one obtains regular evolution equations at the origin.

In terms of the variables introduced above, the hamil-

tonian and momentum constraints become (in vacuum)

$$0 = \mathcal{C}_h = -\partial_r D_B + \frac{D_B}{2} \left( D + \frac{D_B}{2} \right) + AK_B(2K - 3K_B) + \frac{1}{r}(D - D_B - \lambda), \quad (6.5)$$

$$0 = \mathcal{C}_m = -\partial_r K_B + (K - 3K_B) \left[ \frac{D_B}{2} + \frac{1}{r} \right]. \quad (6.6)$$

Notice that the hamiltonian constraint is regular, while the momentum constraint still has the term  $(K - 3K_B)/r \equiv (K_A - K_B)/r$  which has to be handled with care numerically. This is not a problem as the momentum constraint does not feed back into the ADM evolution equations. On the other hand, when one adds multiples of the momentum constraint to the evolution equations in order to obtain hyperbolic reformulations (as in the following section), the regularization procedure requires some of the dynamical variables to be redefined by adding to them a term proportional to  $\lambda$  (see [31] for details). This redefinition, however, does not affect the characteristic structure of the system. Because of this, in the following analysis we will simply ignore this issue.

For the evolution of the gauge, we will again take the Bona-Masso slicing condition and the generalized harmonic shift condition, which in spherical symmetry take the following form

$$\partial_t \alpha = \alpha^2 (\sigma D_\alpha - f K), \quad (6.7)$$

$$\partial_t \sigma = \alpha \left[ \sigma d_\sigma - \frac{D_\alpha}{A} + h \left( \frac{D}{2A} + \sigma K - \frac{2}{rA} \right) \right]. \quad (6.8)$$

The evolution equations for  $D_\alpha$  and  $d_\sigma$  can be obtained directly from the above equations. There is an important comment to be made here about the  $1/r$  term appearing in the evolution equation for  $\sigma$ . This term comes directly from the expression for  ${}^{(3)}\Gamma^r$  and is clearly singular, so the evolution equation for the shift is ill behaved at the origin. This shows an important weakness of the generalized harmonic shift condition: For singular coordinate systems, such as spherical coordinates, the contracted Christoffel symbols can easily be themselves singular. The origin of this problem is in the fact that spherical coordinates  $(r, \theta, \phi)$  are not harmonic even in the case of an Euclidean space. In order to proceed with our study we therefore must remove the offending  $1/r$  term by hand and use instead for  $\sigma$  the following evolution equation

$$\partial_t \sigma = \alpha \left[ \sigma d_\sigma - \frac{D_\alpha}{A} + h \left( \frac{D}{2A} + \sigma K \right) \right]. \quad (6.9)$$

Having to remove the singular term by hand is unfortunate, but as it is a lower order term removing it will not affect the characteristic structure of the system. Still, this calls attention to the fact that the generalized harmonic shift condition might work best for regular coordinate systems like Cartesian coordinates in 3D.

For the evolution equations of the metric components  $A$  and  $B$  we have

$$\partial_t A = 2\alpha A \left[ \sigma \left( D_\alpha + \frac{D}{2} + D_B \right) + d_\sigma - K + 2K_B \right], \quad (6.10)$$

$$\partial_t B = 2\alpha B \left[ \sigma \left( \frac{D_B}{2} + \frac{1}{r} \right) - K_B \right]. \quad (6.11)$$

The evolution equations for  $D$  and  $D_B$  again follow trivially from here.

Finally, the ADM evolution equations for the extrinsic curvature components turn out to be

$$\begin{aligned} \partial_t K &= \frac{\alpha}{A} \left\{ -\partial_r D_\alpha - 2\partial_r D_B + \sigma A \partial_r K \right. \\ &\quad + D_\alpha \left( \frac{D}{2} - D_\alpha \right) + D_B \left( D + \frac{D_B}{2} \right) \\ &\quad \left. + AK^2 - \frac{2}{r}(D_\alpha - D + D_B + \lambda) \right\}, \end{aligned} \quad (6.12)$$

$$\begin{aligned} \partial_t K_B &= \frac{\alpha}{A} \left\{ -\frac{\partial_r D_B}{2} + \sigma A \partial_r K_B - \frac{D_\alpha D_B}{2} + \frac{DD_B}{4} \right. \\ &\quad \left. + AKK_B - \frac{1}{r} \left( D_\alpha - \frac{D}{2} + D_B + \lambda \right) \right\}. \end{aligned} \quad (6.13)$$

Notice that these are directly the standard ADM evolution equations written in terms of  $\{K, K_B\}$ , with no multiples of the constraints added to them. In the next section we will consider how such adjustments affect the hyperbolicity of the full system.

## B. Adjustments and hyperbolicity

In order to analyze the characteristic structure of the full system of evolution equations including the gauge conditions, we start by defining the following vectors

$$\vec{u} := (\alpha, \sigma, A, B, \lambda), \quad (6.14)$$

$$\vec{v} := (D_\alpha, d_\sigma, D, D_B, K, K_B). \quad (6.15)$$

The system of equations can then be written in the form (4.1)-(4.2). It turns out that by doing this, one finds that the ADM evolution system introduced above is not strongly hyperbolic when  $f = 1$  and/or  $h = 1$ . This is undesirable, as these cases correspond precisely to purely harmonic coordinates.

Following [28], in order to obtain strongly hyperbolic systems we will consider adjustments to the evolution equations of the extrinsic curvature components  $K$  and  $K_B$  of the form

$$\partial_t v_i + \sum_{j=1}^m A_{ij} \partial_r v_j + h_i \frac{\alpha}{A} C_h = q_i. \quad (6.16)$$

Note that we are considering only very restricted adjustments here. In particular, we do not modify the evolution equations for the  $D$ 's and for  $d_\sigma$ . As explained in Ref. [28], this is important for the blowup analysis in the next section, as otherwise the constraints that link the  $D$ 's to derivatives of the  $u$ 's will fail to hold and the analysis breaks down [34].

Furthermore, for simplicity we will not consider adjustments that use the momentum constraint. For the coefficients  $h_K$  and  $h_{K_B}$  we make the following ansatz

$$h_K = -2 + b(\alpha, \sigma, A, B), \quad (6.17)$$

$$h_{K_B} = [c(\alpha, \sigma, A, B) - 1]/2. \quad (6.18)$$

With these adjustments we find that the characteristic matrix for our system of evolution equations becomes

$$\mathbf{A} = \alpha \begin{pmatrix} -\sigma & 0 & 0 & 0 & f & 0 \\ 1/A & -\sigma & -h/2A & 0 & -h\sigma & 0 \\ -2\sigma & -2 & -\sigma & 0 & 2 & -8 \\ 0 & 0 & 0 & -\sigma & 0 & 2 \\ 1/A & 0 & 0 & b/A & -\sigma & 0 \\ 0 & 0 & 0 & c/2A & 0 & -\sigma \end{pmatrix}. \quad (6.19)$$

One may now readily verify that this matrix has the following eigenvalues

$$\lambda_\pm^f = \alpha \left( -\sigma \pm \sqrt{f/A} \right), \quad (6.20)$$

$$\lambda_\pm^h = \alpha \left( -\sigma \pm \sqrt{h/A} \right), \quad (6.21)$$

$$\lambda_\pm^c = \alpha \left( -\sigma \pm \sqrt{c/A} \right). \quad (6.22)$$

The system is therefore hyperbolic for  $\{f, h, c\} > 0$ . Furthermore, there exists a complete set of eigenvectors as long as  $c \neq f$  and  $c \neq h$ , so the system is strongly hyperbolic except in those two cases. The eigenfields turn out to be:

$$w_\pm^f = (c - f) D_\alpha - b f D_B \pm \sqrt{fA} [(c - f) K - 2bK_B], \quad (6.23)$$

$$w_\pm^h = (c - h) \left\{ A^{1/2} \left[ d_\sigma - (1 \pm \sigma\sqrt{hA}) K \right] \mp \sqrt{h} \frac{D}{2} \right\} \pm \sqrt{h} \left[ b \left( 1 \pm \sigma\sqrt{hA} \right) - 2c \right] D_B + 2\sqrt{A} \left[ b \left( 1 \pm \sigma\sqrt{hA} \right) - 2h \right] K_B, \quad (6.24)$$

$$w_\pm^c = \sqrt{c} D_B \pm 2\sqrt{A} K_B. \quad (6.25)$$

It is clear from these expressions that when  $c = f$  the first and third pairs of eigenfields become proportional to each other and are hence no longer independent, while for  $c = h$  it is the second and third pairs that become proportional.

### C. Gauge and constraint shocks

As we did for the 1+1 dimensional system, we will now study the possible formation of blowups for the evolution equations in spherical symmetry. In order to apply

the source criteria for avoiding blowups we need to calculate the quadratic source terms in the evolution equations for the eigenfields. We first look for “gauge shocks”, for which we concentrate on the gauge eigenfields  $w_\pm^f$  and  $w_\pm^h$ . For the quadratic source terms we find

$$c_{\pm\pm\pm}^{fff} \propto \frac{1}{(c - f)} \left( 1 - f - \frac{\alpha f'}{2} \right), \quad (6.26)$$

$$c_{\pm\pm\pm}^{hhh} \propto \frac{1}{(c - h)} \frac{\partial h}{\partial \sigma}. \quad (6.27)$$

Demanding now that these terms vanish we obtain precisely the same conditions on  $f$  and  $h$  as in the 1+1 dimensional case. So again  $f = 1 + \text{const}/\alpha^2$  and  $h = h(\alpha)$  are shock avoiding solutions. Furthermore, if one chooses  $f = h = 1 + \text{const}/\alpha^2$ , mixed terms of the form  $w_\pm^f w_\pm^h$  do not appear in the evolution equations of the gauge eigenfields  $w_\pm^f$  and  $w_\pm^h$ , so this is a preferred choice.

In contrast to the 1+1 dimensional case, now also blowups associated with the constraint eigenpair  $w_\pm^c$  can arise. The quadratic coefficient in this case takes the form

$$c_{\pm\pm\pm}^{ccc} \propto (1 - 4b + 3c), \quad (6.28)$$

and by asking for this coefficient to vanish we find

$$b = (1 + 3c)/4. \quad (6.29)$$

From (6.17) and (6.18) we then infer that  $h_K$  and  $h_{K_B}$  are related by

$$h_K = -1 + \frac{3h_{K_B}}{2}, \quad h_{K_B} > -\frac{1}{2}, \quad (6.30)$$

which is the precisely the same constraint shock avoiding half-line in the  $\{h_K, h_{K_B}\}$  parameter space that was found in Ref. [28].

### D. Numerical examples

We will now test the effects of the generalized harmonic shift in spherical symmetry by performing a series of numerical simulations. As in the 1+1 dimensional case, we will concentrate on two aspects, namely the effect of the shift condition on the evolution of the metric, and the possible formation of blowups. Furthermore, in order to decouple geometric effects associated with the center of symmetry, we will consider two distinct regimes, one far from the origin and one close to it.

#### 1. Pulses far from the origin

We will first consider simulations that are far from the origin, using initial data that is similar to the one used in Sec. V C. We start with the Minkowski spacetime, but

use a non-trivial initial slice with a profile  $t_M = p(r_M)$ . The initial metric and extrinsic curvature then become

$$A(t=0) = 1 - p'^2, \quad (6.31)$$

$$B(t=0) = 1, \quad (6.32)$$

$$K(t=0) = -\frac{1}{\sqrt{A}} \left( \frac{p''}{A} + \frac{2p'}{r} \right), \quad (6.33)$$

$$K_B(t=0) = -\frac{p'}{r\sqrt{A}}. \quad (6.34)$$

The profile function  $p(x)$  is again chosen to be a Gaussian,

$$p(r) = \kappa \exp \left[ -\left( \frac{r - r_c}{s} \right)^2 \right], \quad (6.35)$$

using for its amplitude and width the values  $\kappa = \pm 5$  and  $s = 10$ . The center of the Gaussian is taken at  $r_c = 250$ , such that for evolution times of  $t \sim 100$  the perturbation will remain away from the origin.

We have performed runs with the code described in [31], which uses a method of lines with fourth order Runge-Kutta integration in time, and standard second order centered differences in space. We used 5,000 grid points and a grid spacing of  $\Delta r = 0.1$  (which places the outer boundary at 500) together with a time step of  $\Delta r/4$ .

In a preparatory experiment, we studied which evolution systems perform best for our optimal gauge choice  $f = h = 1$ . The upper panel of Fig. 7 (which should be compared with Fig. 7 of [28]) shows the rms of the hamiltonian constraint at time  $t = 100$  as a function of the adjustment parameters  $h_K$  and  $h_{K_B}$ . We can see that the line (6.30) obtained by the source criteria is numerically preferred, although there seems to be a slight discrepancy (in particular for large values of  $c$ ), which is due to the effect of  $1/r$  terms. Removing these terms by hand eliminates this discrepancy. It is important to point out that, in contrast to Ref. [28], the initial data used here satisfies the constraints and all subsequent constraint violations are caused by truncation error.

In order to determine which points on this line perform best, i.e. to fix the eigenspeeds  $\lambda_{\pm}^c$  of the constraint mode, we tested different (constant) values of  $c$ . From the lower panel of Fig. 7 (to be compared with Fig. 5 of [28]) we find that values  $c \sim 1/4$  and  $c \gg 1$  are preferred. This observation can be readily understood by the fact that the system is not strongly hyperbolic for  $c = 0$  and  $c = 1$ , and by the fact that for  $c \sim 1$  we expect contributions from mixed source terms, since then  $w_{\pm}^f$ ,  $w_{\pm}^h$  and  $w_{\pm}^c$  propagate with similar or even identical eigenspeeds.

For our main experiment regarding gauge effects, we concentrated on evolution systems which belong to the shock avoiding family  $h_K = -1 + 3h_{K_B}/2$ , where for  $c$  we considered three different values:  $c = \{1/4, 1, 4\}$ . As long as the pulses remain far from the origin, we have found that the evolutions behave in a very similar way to those of the 1+1 dimensional case described in Sec. V C.

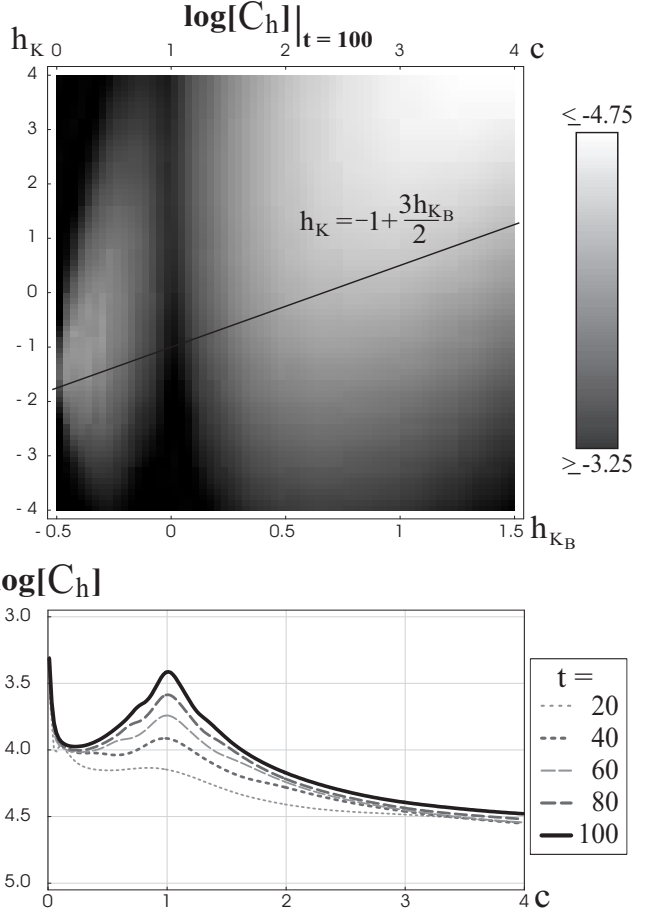


FIG. 7: *Top.* Contour plot of the rms of the hamiltonian constraint at time  $t = 100$  as a function of the adjustment parameters  $h_K$  and  $h_{K_B}$ . The parameter line suggested by the source criteria,  $h_K = -1 + 3h_{K_B}/2$  with  $h_{K_B} > -1/2$ , is shown as a solid line. *Bottom.* For reasons described in the text, along this line  $c \sim 1/4$  and  $c \gg 1$  are preferred values for  $c$ , the latter determining the eigenspeeds  $\lambda_{\pm}^c$  of the constraint mode.

We summarize these results in Fig. 8, showing for these three choices of  $c$  the rms of the hamiltonian constraint at time  $t = 100$  as a function of  $f$  and  $h$ . These graphs are very similar to Fig. 6 and show that  $f = 1$  together with  $h = 1$  or  $h \gg 1$ , and  $f = h$  are again preferred parameter choices, indicating that the same mechanisms as in the 1+1 dimensional case are at work. One should observe the different scales when comparing the three plots corresponding to different values of  $c$ , which indicate that by far the lowest constraint violations are found when the constraint eigenspeed is different from the gauge eigenspeeds.

When the pulses come close to the origin, however, additional effects arise due to  $1/r$  terms. In the next section we will consider this situation.

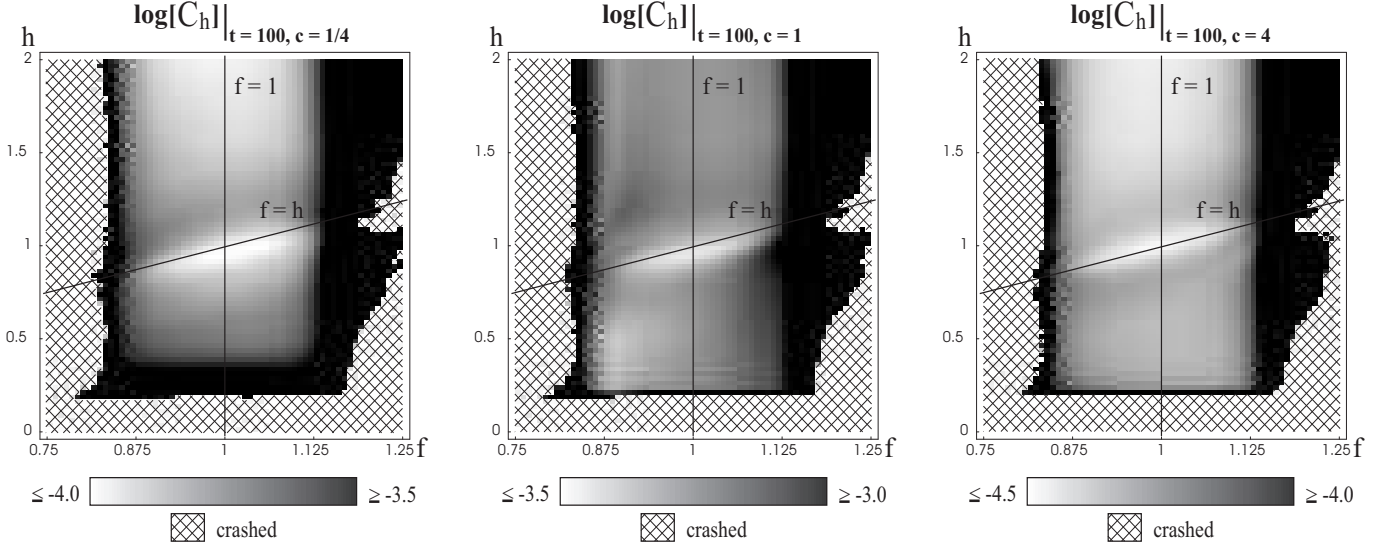


FIG. 8: Contour plot of the rms of the hamiltonian constraint at time  $t = 100$ . As in the 1+1 dimensional case, again  $f = 1$  together with  $h = 1$  or  $h \gg 1$ , and  $f = h$  are preferred parameter choices. Furthermore, by far the lowest constraint violations are found when the constraint eigenspeed is different from the gauge eigenspeeds, i.e. for  $c \neq 1$ .

## 2. Pulses close to the origin

In order to see directly the effect of the generalized harmonic shift condition on the evolution of the geometric variables, we will consider a series of simulations of the Minkowski spacetime, but this time close to the origin  $r = 0$ . The initial data for these runs will be simpler than the one used in the previous section: We start with a flat Minkowski slice with  $A = B = 1$  and  $K_A = K_B = 0$ , and take a non-trivial initial lapse of the form

$$\alpha = 1 + \kappa r^2 \exp \left[ - \left( \frac{r - r_c}{s} \right)^2 \right], \quad (6.36)$$

with  $\kappa = 10^{-5}$ ,  $r_c = 10$  and  $s = 1$ . All simulations shown here use 4,000 grid points, with a grid spacing of  $\Delta r = 0.01$  (which places the outer boundary at  $r = 40$ ), together with a time step of  $\Delta r/4$ . In the plots, the initial data is shown as a dashed line and the final values at  $t = 20$  as a solid line. Intermediate values are plotted every  $\Delta t = 2$  in light gray.

As reference, we first show in Fig. 9 a run for the case of harmonic slicing ( $f = 1$ ) with no shift. As expected, the perturbation pulse in the lapse separates into two pulses, one moving outward and one inward. The inward moving pulse goes through the origin and starts moving out much in the way a simple scalar wave would. The pulses in the lapse are accompanied by similar pulses in the metric variables  $A$  and  $B$ .

Next we consider the same situation, but now using a harmonic shift with  $h = 1$ . Fig. 10 shows results from this run. The lapse behaves in exactly the same way as before, but now there is a non-trivial shift. The evolution of  $\sigma$  indicates that the shift behaves much in the same way as the lapse, with two pulses traveling in opposite

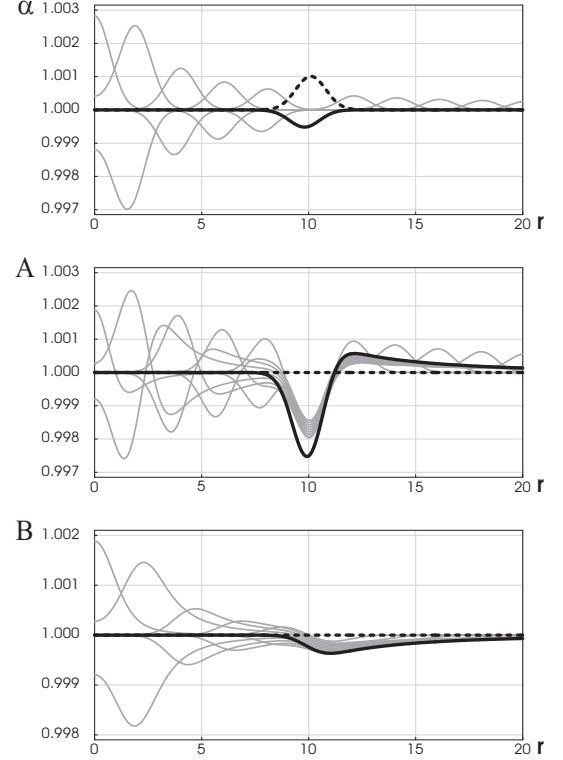


FIG. 9: Evolution of pulses close to the origin for harmonic slicing ( $f = 1$ ) and zero shift.

directions, with the inward moving pulse going through the origin and then moving out as expected. However, the evolution of the metric variables  $A$  and  $B$  already shows a very strange behavior after the pulses in  $\alpha$  and  $\sigma$  have passed through the origin. First, notice how the

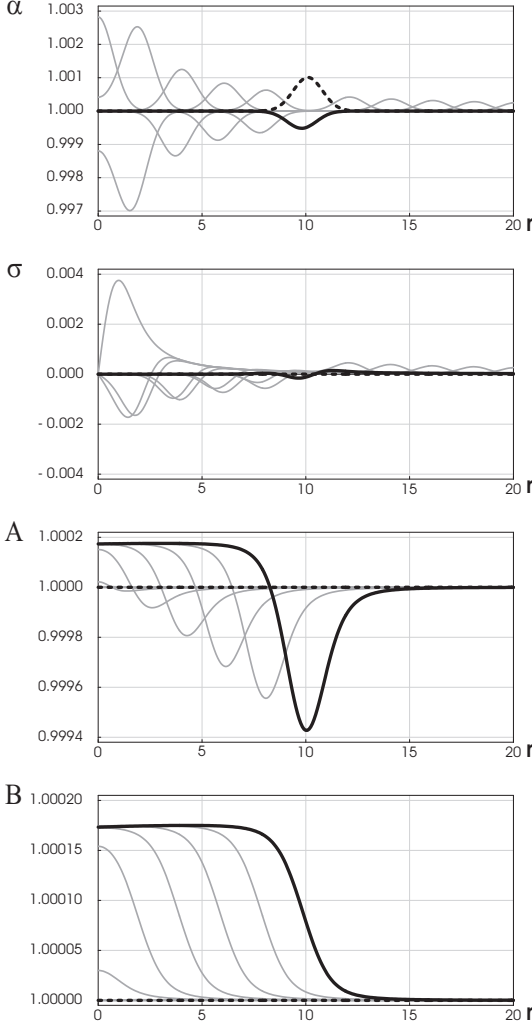


FIG. 10: As previous plot, but using the harmonic shift condition with  $h = 1$ .

metric variables do not return back to trivial values, but rather seem to settle into non-trivial constant values in the region behind the pulses. More worrying still is the fact that as the pulse in  $A$  moves away from the origin, it becomes larger and larger in size (making  $A$  move toward zero), instead of decaying as  $1/r$  as would be expected from spherical waves. This already indicates that the harmonic shift condition might not be well adapted to spherical coordinates. In fact, if the simulation is continued somewhat further, the pulse in the shift also starts to grow following the growth in  $A$ .

Fig. 11 shows a similar run, but now using  $f = 1$  and  $h = 2$ . The whole simulation behaves much the same way as before, except for the fact that the shift now shows evidence of two pulses separating and traveling at different speeds after the rebound through the origin. If the simulation is followed for longer, the faster moving pulse shows again growth in the metric function  $A$  and in  $\sigma$  as it moves.

Finally, in Fig. 12 we show a simulation with  $h = 1$  for

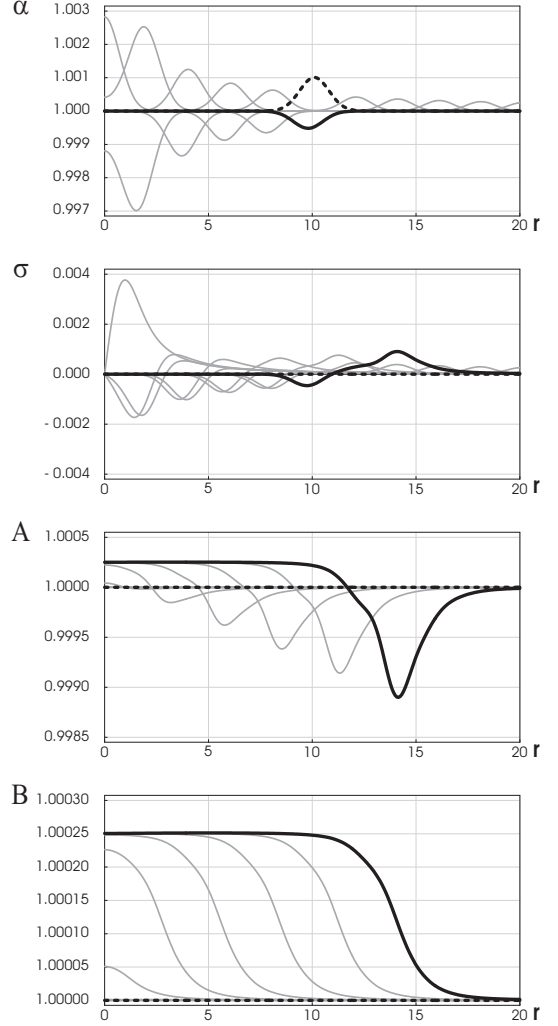


FIG. 11: Same as previous plots, but now using the generalized harmonic shift with  $h = 2$ .

a case where we have left the lapse equal to one throughout the evolution. The initial data in this case is purely Minkowski data with a shift of the form

$$\sigma = 1 + \kappa r^2 \exp \left[ - \left( \frac{r - r_c}{s} \right)^2 \right], \quad (6.37)$$

with  $\kappa = 10^{-4}$ ,  $s = 1$  and  $r_c = 5$ . The purpose of this run is to decouple the harmonic shift condition from the slicing condition. The figure shows very dramatically how both the radial metric function  $A$  and the shift  $\sigma$  grow as the pulses move out.

The growth we have seen associated with outward moving shift pulses in the simulations discussed above is not only highly counter-intuitive, it is also undesirable as it eventually causes serious problems with the simulation as  $A$  gets too close to zero and  $\sigma$  becomes too large. The whole pattern indicates that the harmonic shift condition is in fact ill-adapted to spherical coordinates.

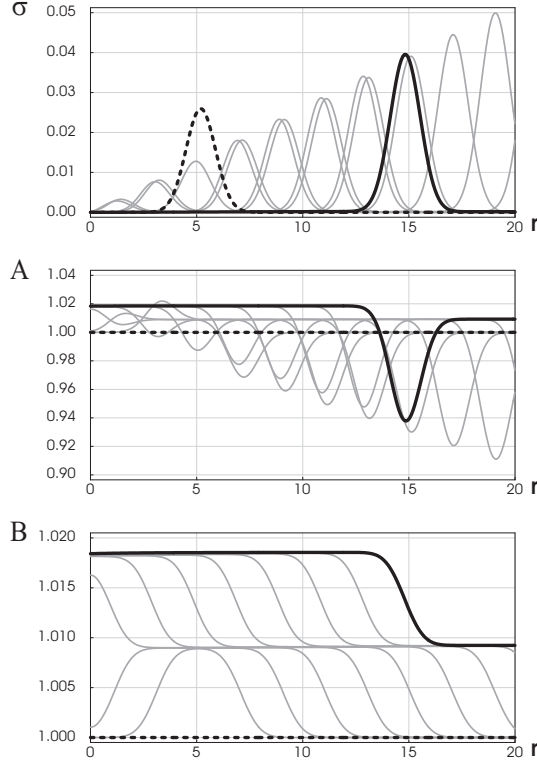


FIG. 12: Trivial Minkowski slices where the lapse remains equal to unity, together with the harmonic shift condition ( $h = 1$ ).

## VII. DISCUSSION

We have proposed a natural generalization of the condition for harmonic spatial coordinates analogous to the generalization of harmonic time slices of Bona *et al.* [19]. This coordinate condition implies a condition for the shift that has the form of an evolution equation for the shift components. We have found that if one wants to decouple this evolution equation for the shift from the slicing condition, it is important to work with a rescaled shift vector  $\sigma^i = \beta^i/\alpha$ .

We have also shown that the evolution equation for the shift proposed here can be seen to lead to fully hyperbolic evolution systems both in the case of 1+1 “toy” relativity and in the case of spherical symmetry. Though we have not done a completely general analysis here, it is to be expected that it will also lead to fully hyperbolic systems in the 3D case. Here we have concentrated on simple one-dimensional systems in order to take the hyperbolicity analysis further and study the possible formation of blowups associated with this shift condition. We find that the coefficient controlling the gauge speed associated with the shift must itself be independent of  $\sigma$  in order to avoid blowups. In the slicing and constraint sectors we recover previous results found in [28].

We have also performed a series of numerical simulation both to confirm the predictions of the blowup analy-

sis, and to study what effect the shift has on the evolution of the geometric variables. In the 1+1 dimensional case, we find that the effect of the shift is to take the spatial metric back to a trivial value everywhere, by propagating away any non-trivial values in a wavelike fashion.

In spherical symmetry the situation is considerably more complex. In the first place, we find that the generalized harmonic shift condition is singular at  $r = 0$ . This is not surprising as it is well known that spherical coordinates are not harmonic even for Euclidean space (the harmonic condition in this case is in fact ill defined at the origin). In order to go further we therefore removed the offending singular term by hand, which still leaves us with a non-trivial hyperbolic shift condition. What we have found from the simulations is that, in spite of having removed the singular term, the shift condition still behaves in a pathological way close to the origin: As pulses in the shift pass through the origin and rebound, the metric components  $A$  and  $B$  do not return back to their trivial Minkowski values. Worse, as these pulses move out, the perturbation in  $A$  grows instead of decaying (with negative sign, making  $A$  approach zero), while the shift  $\sigma$  becomes larger and larger. This behavior is not only counter-intuitive (one expects spherical waves to become smaller as they move away from the origin), but it also eventually causes serious problems with the evolution. It would therefore seem that the generalized harmonic shift condition is simply not well adapted to spherical coordinates: It would seem that we are asking for the coordinates to be driven toward a situation that can simply not be reached, so the evolution becomes pathological.

However, as the harmonic shift condition is clearly not 3-covariant, and as it seems to work in the 1+1 dimensional case, it might very well be that it also behaves well in full 3D simulations using Cartesian coordinates. We are currently investigating this issue and will report on our results elsewhere.

As a final note, since we have found the generalized harmonic shift condition to be not well adapted to spherical coordinates, we believe that it is important to look for shift conditions that are 3-covariant and give us the same shift vector regardless of the spatial coordinates one uses. This requirement of 3-covariance is in fact not satisfied by some recently proposed shift conditions that are currently being used by large scale 3D simulations, such as the “Gamma driver” shift [3, 32, 33]. We are currently also studying ways to write hyperbolic 3-covariant shift conditions.

## Acknowledgments

It is a pleasure to thank Sascha Husa for many useful discussions and comments. This work was supported in part by DGAPA-UNAM through grants IN112401, IN122002 and IN119005 and by DFG grant “SFB Transregio 7: Gravitationswellenastronomie”. B.R. ac-

knowledges financial support from the Richard-Schieber Stiftung. All runs were made at the `ekbek` linux cluster in the “Laboratorio de Super-Cómputo Astrofísico (La-SumA)”, CINVESTAV, built through CONACyT grant 42748.

## APPENDIX A: GENERALIZED HARMONIC LAPSE AND SHIFT CONDITIONS

Here we will provide a general derivation of equations (3.1) and (3.6) for the lapse and shift. Let us start by considering the d’Alambertian of any number  $a$  of functions  $\psi^a(x^\mu)$  with their corresponding source terms

$$\square\psi^a = S^{\psi^a}. \quad (\text{A1})$$

Now, the d’Alambertian can be written in general as

$$\square\psi^a = \frac{1}{\sqrt{-g}} \partial_\mu [\sqrt{-g} g^{\mu\nu} \partial_\nu \psi^a]. \quad (\text{A2})$$

Using  $g^{\mu\nu} = \gamma^{\mu\nu} - n^\mu n^\nu$ , with  $\gamma^{\mu\nu}$  the projector operator on the hypersurfaces  $\Sigma_t$  with normal  $n^\mu$ , we find

$$\begin{aligned} \square\psi^a &= \frac{1}{\alpha\sqrt{\gamma}} \partial_\mu [\alpha\sqrt{\gamma} \gamma^{\mu\nu} \partial_\nu \psi^a] \\ &- \frac{1}{\alpha\sqrt{\gamma}} \partial_\mu [\alpha\sqrt{\gamma} n^\mu n^\nu \partial_\nu \psi^a], \end{aligned} \quad (\text{A3})$$

where we used the fact that  $g := \det g_{\mu\nu} = -\alpha^2\gamma$  with  $\gamma := \det \gamma_{ij}$  the determinant of the 3-metric on  $\Sigma_t$ . We then have

$$\begin{aligned} \square\psi^a &= {}^3\Delta\psi^a + a^\mu \nabla_\mu \psi^a + K n^\mu \nabla_\mu \psi^a \\ &- n^\mu \nabla_\mu (n^\nu \nabla_\nu \psi^a), \end{aligned} \quad (\text{A4})$$

where  ${}^3\Delta$  is the Laplacian compatible with the 3-metric  $\gamma_{ij}$ ,  $a^\mu = n^\nu \nabla_\nu n^\mu \equiv \gamma^{\mu\nu} \nabla_\nu [\ln \alpha] =: D^\mu [\ln \alpha]$  is the 4-acceleration of the normal observers, and we used  $K = -\nabla_\nu n^\nu$ .

In order to obtain for instance a system of first order equations one can further define

$$Q^{\mu a} := D^\mu \psi^a, \quad (\text{A5})$$

$$\Pi^a := \mathcal{L}_{\vec{n}} \psi^a = n^\nu \nabla_\nu \psi^a, \quad (\text{A6})$$

where  $D^\mu \psi^a := \gamma^{\mu\sigma} \nabla_\sigma \psi^a$ . Collecting the above results we obtain

$$\mathcal{L}_{\vec{n}} \Pi^a - a_\mu Q^{\mu a} - D_\mu Q^{\mu a} - \Pi^a K = -S^{\psi^a}. \quad (\text{A7})$$

A simple application of the above results is the case when  $\psi^a = x^a$ , in which case  $\Pi^a = n^a = (1, -\beta^i)/\alpha$ ,  $Q_\mu^a = \gamma_\mu^a$ , and  $D_\nu Q^{\nu i} = \partial_j (\sqrt{\gamma} \gamma^{ij})/\sqrt{\gamma} \equiv -{}^3\Gamma^i$ . The above equation with  $S^{\psi^a} = 0$  is then called the *harmonic coordinate condition*, which provides an evolution equation for the lapse - Eq. (2.9) - and for the shift - Eq. (2.10) - when taking  $x^a = (t, x^i)$  with  $t$  defining the time slicings and  $x^i$  being spatial coordinates on  $\Sigma_t$ .

On the other hand one can take  $\square\psi^a = S^{\psi^a}$  with a source term of the form  $S^{\psi^a} = q_{\psi^a} n^\mu n^\nu \nabla_\mu \nabla_\nu \psi^a$  (no sum over index  $a$ ). Now, using  $n^\mu n^\nu = \gamma^{\mu\nu} - g^{\mu\nu}$ , one obtains

$$n^\mu n^\nu \nabla_\mu \nabla_\nu \psi^a = \gamma^{\mu\nu} \nabla_\mu \nabla_\nu \psi^a - \square\psi^a. \quad (\text{A8})$$

Using the orthogonal decomposition  $\nabla_\nu \psi^a = D_\nu \psi^a - n_\nu n_\sigma \nabla^\sigma \psi^a = Q_\nu^a - n_\nu \Pi^a$  we find

$$n^\mu n^\nu \nabla_\mu \nabla_\nu \psi^a = D_\nu Q^{\nu a} + \Pi^a K - \square\psi^a, \quad (\text{A9})$$

where we used  $\gamma^{\mu\sigma} \nabla_\mu n_\sigma = \nabla_\mu n^\mu = -K$  and  $\gamma^{\mu\nu} n_\nu \equiv 0$ . In this way the equation  $\square\psi^a = S^{\psi^a}$  becomes

$$\square\psi^a = \frac{q_{\psi^a}}{1 + q_{\psi^a}} (D_\nu Q^{\nu a} + \Pi^a K). \quad (\text{A10})$$

Finally,  $-\square\psi^a$  is given by the left hand side of Eq. (A7), from where we find

$$\begin{aligned} \mathcal{L}_{\vec{n}} \Pi^a - a_\mu Q^{\mu a} - D_\mu Q^{\mu a} - \Pi^a K &= \\ -\frac{q_{\psi^a}}{1 + q_{\psi^a}} (D_\nu Q^{\nu a} + \Pi^a K), \end{aligned} \quad (\text{A11})$$

which simplifies to

$$\mathcal{L}_{\vec{n}} \Pi^a - a_\mu Q^{\mu a} = \frac{1}{1 + q_{\psi^a}} (D_\nu Q^{\nu a} + \Pi^a K). \quad (\text{A12})$$

In this way by taking  $\psi^a = (t, x^i)$ ,  $q_t = a_f = 1/f - 1$ ,  $q_{x^i} = a_h = 1/h - 1$ , together with Eqs. (A5) and (A6) (leading to  $\Pi^a = n^a = (1, -\beta^i)/\alpha$  and  $Q_\mu^a = \gamma_\mu^a$ ), one recovers the evolution equations (3.1) and (3.6) for  $\alpha$  and  $\beta^i$ , respectively.

## APPENDIX B: METRIC AND CHRISTOFFEL SYMBOLS IN 3+1 LANGUAGE

For the expression of the generalized harmonic gauge conditions one needs to write the 4-metric of spacetime and its associated Christoffel symbols in 3+1 language. The 4-metric in terms of 3+1 quantities has the form

$$g_{00} = -(\alpha^2 - \gamma_{ij} \beta^i \beta^j), \quad (\text{B1})$$

$$g_{0i} = \gamma_{ij} \beta^j, \quad (\text{B2})$$

$$g_{ij} = \gamma_{ij}, \quad (\text{B3})$$

and the corresponding inverse metric is

$$g^{00} = -1/\alpha^2, \quad (\text{B4})$$

$$g^{0i} = \beta^i/\alpha^2, \quad (\text{B5})$$

$$g^{ij} = \gamma^{ij} - \beta^i \beta^j / \alpha^2. \quad (\text{B6})$$

From this one can obtain the following expressions for

the 4-Christoffel symbols in terms of 3+1 quantities

$$\Gamma_{00}^0 = (\partial_t \alpha + \beta^m \partial_m \alpha - \beta^m \beta^n K_{mn}) / \alpha, \quad (\text{B7})$$

$$\Gamma_{0i}^0 = (\partial_i \alpha - \beta^m K_{im}) / \alpha, \quad (\text{B8})$$

$$\Gamma_{ij}^0 = -K_{ij} / \alpha, \quad (\text{B9})$$

$$\begin{aligned} \Gamma_{00}^l &= \alpha \partial^l \alpha - 2\alpha \beta^m K_m^l \\ &\quad - \beta^l (\partial_t \alpha + \beta^m \partial_m \alpha - \beta^m \beta^n K_{mn}) / \alpha \\ &\quad + \partial_t \beta^l + \beta^m {}^{(3)}\nabla_m \beta^l, \end{aligned} \quad (\text{B10})$$

$$\begin{aligned} \Gamma_{m0}^l &= -\beta^l (\partial_m \alpha - \beta^n K_{mn}) / \alpha \\ &\quad - \alpha K_m^l + {}^{(3)}\nabla_m \beta^l, \end{aligned} \quad (\text{B11})$$

$$\Gamma_{ij}^l = {}^{(3)}\Gamma_{ij}^l + \beta^l K_{ij} / \alpha. \quad (\text{B12})$$

The contracted Christoffel symbols  $\Gamma^\alpha := g^{\mu\nu} \Gamma_{\mu\nu}^\alpha$  then become

$$\Gamma^0 = -\frac{1}{\alpha^3} (\partial_t \alpha - \beta^m \partial_m \alpha + \alpha^2 K) \quad (\text{B13})$$

and

$$\begin{aligned} \Gamma^i &= \frac{\beta^i}{\alpha^3} (\partial_t \alpha - \beta^m \partial_m \alpha + \alpha^2 K) + {}^{(3)}\Gamma^i \\ &\quad - \frac{1}{\alpha^2} (\partial_t \beta^i - \beta^m \partial_m \beta^i + \alpha \partial^i \alpha). \end{aligned} \quad (\text{B14})$$

---

[1] L. Smarr and J. York, Phys. Rev. D **17**, 1945 (1978).  
[2] L. Smarr and J. York, Phys. Rev. D **17**, 2529 (1978).  
[3] M. Alcubierre, B. Brügmann, P. Diener, M. Koppitz, D. Pollney, E. Seidel, and R. Takahashi, Phys. Rev. D **67**, 084023 (2002), gr-qc/0206072.  
[4] M. Alcubierre, Class. Quantum Grav. **20**, 607 (2003), gr-qc/0210050.  
[5] M. Alcubierre, A. Corichi, J. González, D. Nuñez, and M. Salgado, Class. Quant. Grav. **20**, 3951 (2003), gr-qc/0303069.  
[6] M. Alcubierre, A. Corichi, J. González, D. Nuñez, and M. Salgado, Phys. Rev. D **67**, 104021 (2003), gr-qc/0303086.  
[7] O. Sarbach and M. Tiglio, Phys. Rev. D **66**, 064023 (2002), gr-qc/0205086.  
[8] L. Lindblom and M. A. Scheel, Phys. Rev. D **67**, 124005 (2003), gr-qc/0301120.  
[9] Y. Bruhat, Acta Mathematica **88**, 141 (1952).  
[10] B. Szilagyi, B. Schmidt, and J. Winicour, Phys. Rev. D **65** (2002), gr-qc/0106026.  
[11] D. Garfinkle, Phys. Rev. D **65**, 044029 (2002), gr-qc/0110013.  
[12] F. Pretorius, Class. Quant. Grav. **22**, 425 (2005), gr-qc/0407110.  
[13] C. Bona and J. Massó, Phys. Rev. D **38**, 2419 (1988).  
[14] C. Bona and J. Massó, Phys. Rev. D **40**, 1022 (1989).  
[15] C. Bona and J. Massó, Phys. Rev. Lett. **68**, 1097 (1992).  
[16] A. Abrahams, A. Anderson, Y. Choquet-Bruhat, and J. York, Phys. Rev. Lett. **75**, 3377 (1995), gr-qc/9506072.  
[17] C. Bona, J. Massó, E. Seidel, and J. Stela, Phys. Rev. D **56**, 3405 (1997), gr-qc/9709016.  
[18] A. Geyer and H. Herold, Phys. Rev. D **52**, 6182 (1995).  
[19] C. Bona, J. Massó, E. Seidel, and J. Stela, Phys. Rev. Lett. **75**, 600 (1995), gr-qc/9412071.  
[20] D. Bernstein, Ph.D. thesis, University of Illinois Urbana-Champaign (1993).  
[21] P. Anninos, K. Camarda, J. Massó, E. Seidel, W.-M. Suen, and J. Towns, Phys. Rev. D **52**, 2059 (1995).  
[22] C. Bona and C. Palenzuela, Phys. Rev. D **69**, 104003 (2004), gr-qc/0401019.  
[23] J. York, in *Sources of Gravitational Radiation*, edited by L. Smarr (Cambridge University Press, Cambridge, England, 1979).  
[24] C. Bona and J. Massó, International Journal of Modern Physics C: Physics and Computers **4**, 88 (1993).  
[25] M. Alcubierre, Phys. Rev. D **55**, 5981 (1997), gr-qc/9609015.  
[26] S. Alinhac, *Blowup for Nonlinear Hyperbolic Equations* (Birkhäuser, Boston, U.S.A., 1995).  
[27] F. John, *Partial Differential Equations* (Springer-Verlag, New York, 1986).  
[28] B. Reimann, M. Alcubierre, J. A. González, and D. Nuñez, Phys. Rev. D **71**, 064021 (2005), gr-qc/0411094.  
[29] R. Arnowitt, S. Deser, and C. W. Misner, in *Gravitation: An Introduction to Current Research*, edited by L. Witten (John Wiley, New York, 1962), pp. 227–265.  
[30] M. Alcubierre and J. Massó, Phys. Rev. D **57**, 4511 (1998).  
[31] M. Alcubierre and J. González, Comp. Phys. Comm. **167**, 76 (2005), gr-qc/0401113.  
[32] B. Brügmann, W. Tichy, and N. Jansen, Phys. Rev. Lett. **92**, 211101 (2004), gr-qc/0312112.  
[33] M. Alcubierre et al. (2004), gr-qc/0411149.  
[34] It is in fact possible to lift this restriction, but the analysis would become more involved, and since here we are mostly interested in studying the effects of the generalized harmonic shift condition we prefer not to complicate the analysis any further.